

Angular Dependence of Photoemission and Atomic Orbitals in the Layer Compound  $1T\text{-TaSe}_2$ 

Morton M. Traum, Neville V. Smith, and F. J. Di Salvo

*Bell Laboratories, Murray Hill, New Jersey 07974*

(Received 30 January 1974)

The intensity of photoemission from the Ta-derived  $d$  states in the layer compound  $1T\text{-TaSe}_2$  has been measured as a function of angle at the photon energy 10.2 eV. The dependence of the  $d$  emission on azimuthal angle displays three pairs of major lobes and indications of three pairs of minor lobes. If it is assumed that these photoelectrons are created on Ta atoms, they propagate preferentially along directions which avoid neighboring Se atoms. The relationship with atomic orbitals and with band theory is discussed.

The positions of peaks in the photoelectron energy spectra of solids are often readily explained in terms of densities of states or joint densities of states,<sup>1</sup> i.e., properties which depend only on the energy bands. Peak intensities, on the other hand, present a more difficult problem, but are potentially more informative since they depend on momentum matrix elements and, therefore, on the details of the electronic wave functions. This paper reports measurements of the variation with azimuthal angle of photoemission from the layered compound  $1T\text{-TaSe}_2$ . We concentrate primarily on the intensity of emission from the Ta-derived  $d$  states. It will be seen that the  $d$  emission is consistent with the threefold rotational symmetry of this crystal, and that a simple billiard-ball picture of the observed anisotropies is possible. We argue further that some of the anisotropy can be related to the angular dependence of the atomic Ta  $d$  orbitals.

Our experimental apparatus has been described elsewhere.<sup>2</sup> Its essential feature is a photoelectron energy analyzer which accepts only a small solid angle and can be positioned at various polar angles,  $\theta$ , with respect to the surface normal. The azimuthal angle,  $\varphi$ , is varied by rotating the sample about its surface normal ( $z$  direction). In this paper, we will concentrate on variations with  $\varphi$  for a fixed value of  $\theta$ . The sample was prepared by cleaving in an ultrahigh vacuum of  $1 \times 10^{-10}$  Torr. The sample was illuminated with normally incident photons of energy 10.2 eV.

Figure 1 shows the photoelectron energy spectrum taken on  $1T\text{-TaSe}_2$  at  $\theta = 55^\circ$  and  $\varphi = 0^\circ$ . Relying on previous band-structure schemes<sup>3-5</sup> and on previous photoemission work,<sup>6</sup> we identify the small peak originating from 0.8 eV below the Fermi level as photoemission from the occupied Ta-derived  $d$  states. The larger peaks at lower energy represent emission from the Se-derived  $p$  states. In what follows, the cross-hatched area

in Fig. 1 will be used as a measure of the Ta  $d$  emission.

The outer curve in Fig. 2 is a radial plot representing the variation with  $\varphi$  of the total emission at  $\theta = 55^\circ$ . Since the  $d$  emission is only a small fraction of the total, the outer curve may also be regarded as the intensity of the Se  $p$  emission. The threefold rotational symmetry of the crystal is quite conspicuous. We observe three major lobes centered at the  $\varphi = 0^\circ$ ,  $120^\circ$ , and  $240^\circ$  positions and three minor lobes at  $60^\circ$ ,  $180^\circ$ , and  $300^\circ$ . The inner curve of Fig. 2 represents the intensity of the Ta  $d$  emission. Three pairs of

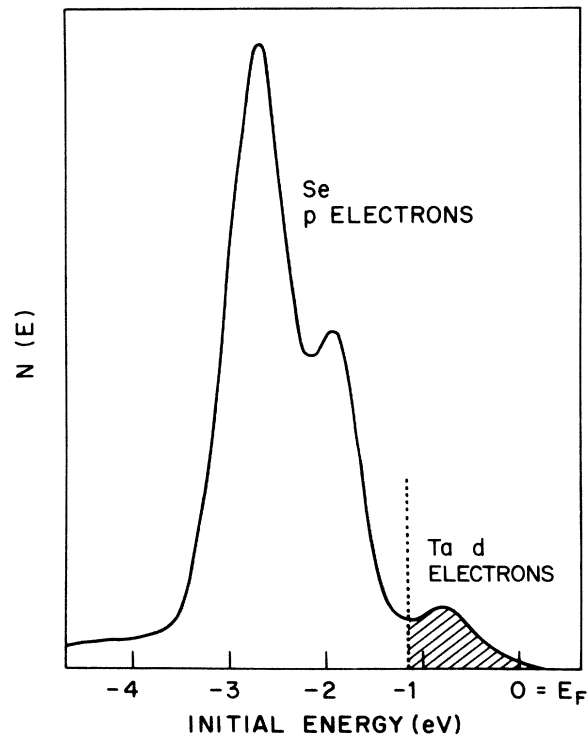


FIG. 1. Energy spectrum of photoelectrons emitted from  $1T\text{-TaSe}_2$  at  $\theta = 55^\circ$  and  $\varphi = 0^\circ$ , referred to initial-state energy taking zero at the Fermi level.

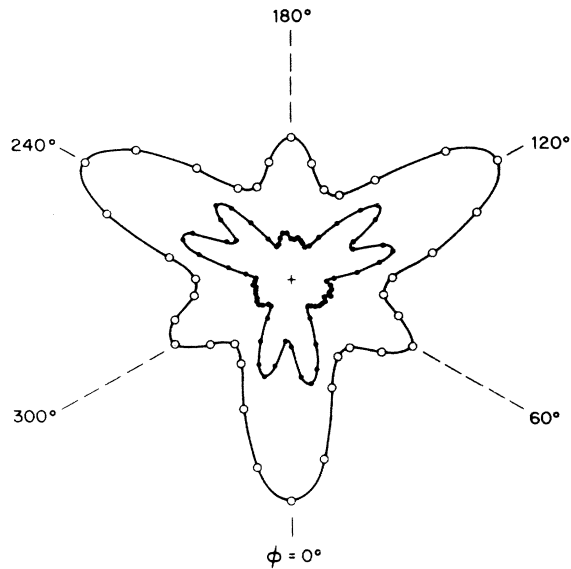


FIG. 2. Radial plots of the azimuthal dependence at  $\theta = 55^\circ$  of the total photoemission intensity (open circles) and, on a  $5 \times$  expanded scale, the  $d$ -emission intensity (full circles). Smooth curves have been drawn to connect the experimental points.

lobes are centered at  $\varphi = 0^\circ$ ,  $120^\circ$ , and  $240^\circ$ , and there are indications of three pairs of minor lobes at  $60^\circ$ ,  $180^\circ$ , and  $300^\circ$ .

An x-ray diffraction study of the sample revealed that the photoemission pattern is oriented with respect to the crystal structure in the manner shown in Fig. 3. The two uppermost atomic sheets are shown, and the Ta  $d$ -emission pattern is centered on a Ta atom. If we adopt a localized picture and assume that these photoelectrons are created on Ta sites, it is seen in Fig. 3 that they then propagate preferentially in the directions between the nearest-neighbor Se atoms rather than along the Ta-Se bonds. Note also that the bifurcation into pairs of lobes corresponds to those trajectories which avoid both the first- and second-nearest Se neighbors. It is as though the Se atoms were opaque to the photoelectrons. This semiclassical billiard ball picture has been confirmed by further experiments on the similar material  $1T$ -TaS<sub>2</sub> where the lobe structure was investigated as a function of  $\theta$ . At low  $\theta$ , the  $d$ -emission intensity is isotropic. At  $\theta \sim 25^\circ$  three broad lobes develop, which then split into pairs as  $\theta$  is increased further.

The photoemission process is usually considered as three sequential steps<sup>1</sup>: (1) optical excitation, (2) transport to the surface, and (3) escape into vacuum. Several explanations of our

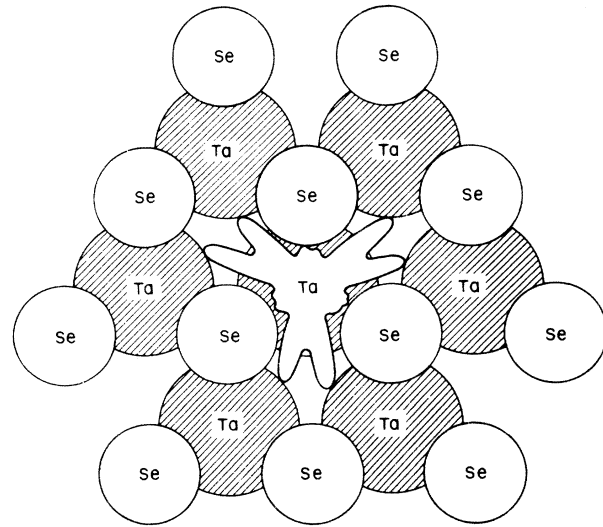


FIG. 3. The experimental Ta  $d$ -emission pattern for  $\theta = 55^\circ$  superposed on the two uppermost atomic sheets of the real-space crystal structure. A third sheet of Se atoms (not shown) completes the Se-Ta-Se sandwich and is the same as the first sheet except for a rotation of  $60^\circ$  about the center Ta atom; the coordination of each Ta atom is close to octahedral. The crystal consists of a succession of such sandwiches.

results are possible depending on which step, or combination of steps, is regarded as the major source of the anisotropies. For example, in the transport step, variations in the electron group velocity could give rise to anisotropies like those observed. Diffraction effects of the kind discussed by McRae<sup>7</sup> in connection with low-energy electron emission and the formation of Kikuchi bands may also be relevant. Mechanisms involving surface states<sup>8</sup> or surface resonances provide additional possibilities. The opaque-billiard-ball picture presented above places the major source of the anisotropy in the transport step, and therefore in the properties of the final states in the optical transitions. In the remainder of the paper, however, we present an alternative model which emphasizes the properties of the initial states and, in particular, the angular dependence of the atomic Ta  $d$  orbitals.

Following an approach used by Gadzuk,<sup>9</sup> we represent an observed photoelectron by the plane wave  $e^{i\vec{p}\cdot\vec{r}}$ . For simplicity, refraction at the boundary and band-structure effects are ignored, and it is assumed that  $e^{i\vec{p}\cdot\vec{r}}$  will serve also as the final-state wave function  $|f\rangle$  in the optical transition which gave rise to the photoelectron. Let us represent the initial-state wave function

as a tight-binding Bloch sum over lattice sites  $\vec{R}_i$ :

$$|i\rangle = \sum_i \exp(i\vec{k} \cdot \vec{R}_i) \varphi(\vec{r} - \vec{R}_i). \quad (1)$$

The  $\varphi(\vec{r})$  represent the appropriate atomic orbitals (or combinations of atomic orbitals). The contribution  $I_k(\vec{p})$  of such a transition to the intensity of photoelectrons emitted with momentum  $\vec{p}$  will be proportional to  $|\langle f | \nabla \cdot \vec{A} | i \rangle|^2$ , where  $\vec{A}$  is the vector potential of the incident radiation. It is then easily shown that

$$I_k(\vec{p}) \propto \sum_{\vec{G}} \delta(\vec{k} - \vec{p} - \vec{G}) |\varphi(\vec{p})|^2, \quad (2)$$

where the summation is over reciprocal lattice vectors,  $\vec{G}$ , and

$$\varphi(\vec{p}) = \int e^{i\vec{p} \cdot \vec{r}} \varphi(\vec{r}) d^3r \quad (3)$$

is simply the momentum representation of an individual atomic orbital. This model is, of course, an oversimplification, particularly at the low photon energy used in our experiments. It is expected that the major assumption of a plane wave form for  $|f\rangle$  will have greater validity at higher photon energies.

The  $\delta$  function in (2) embodies the requirement of  $k$  conservation in the optical transition. This purely band structure effect is considered further in Fig. 4 where we have superposed the radial pattern of the Ta  $d$  emission onto the  $k_x = 0$  plane of the Brillouin zone. The average kinetic energy of the photoelectrons and the known value of  $\sin\theta$  lead to an estimate of the component of  $\vec{p}$  parallel to the surface. The broken circle has been constructed with a radius of this magnitude. We find, in this band picture, that the bulk of the Ta  $d$  emission comes from points in  $k$  space clustered around the points of intersection between this circle and the broken radial lines. Reassuringly, these points fall inside the Fermi surface which consists of electron pockets centered around the  $M$  points as shown.<sup>10</sup>

Because of the weak Van der Waals bonding between layers, the bands in the  $k_x$  direction are expected to be rather flat,<sup>3-5</sup> so that the picture of Fig. 4 will apply even though  $k_x \neq 0$ . Another consequence of this two-dimensionality is that the energy bands will have sixfold rotational symmetry. Although six pairs of lobes appear to be present, the observed symmetry is quite definitely threefold. Returning to Eq. (2), therefore, we must attribute the greater strength of the major lobes to the modulating effect of the  $|\varphi(\vec{p})|^2$  term. It is in this sense that the angular distribution of photoemission reflects the behavior of the atomic

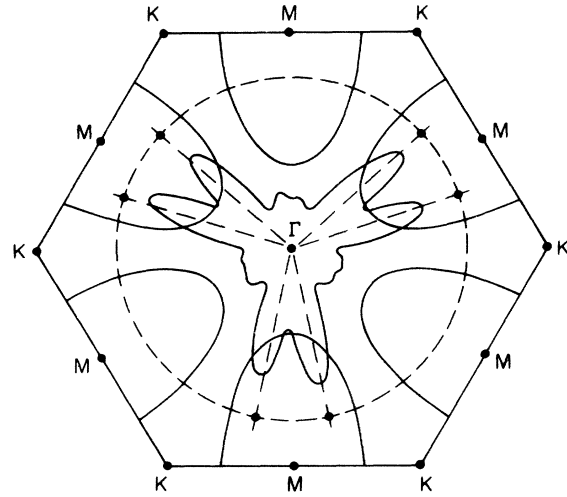


FIG. 4. The experimental Ta  $d$ -emission pattern superposed on the  $\Gamma MK$  plane of the Brillouin zone. The points of intersection between the broken circle and the broken radial lines represent the estimated mean  $k$ -space locations of the optical transitions contributing to the major lobes.

orbitals. Referring back to Fig. 3, we conclude that the atomic Ta  $d$  orbitals should have their momentum density piled up in the directions between the nearest neighbor Se atoms rather than along the Ta-Se bonds. This is consistent with the currently accepted nonbonding character of the  $d$  states in such layer materials.<sup>3-5</sup> Using  $sd^3$  hybrid orbitals appropriate to the local octahedral ligand field,<sup>11</sup> we are able to predict qualitatively the strong weighting of the emission in directions between the neighboring Se atoms, but, interestingly, are unable to predict the bifurcation into pairs of lobes as observed. It appears that the bifurcation is not a ligand-field effect on the orbitals, but is rather an effect whose ultimate explanation will require a detailed understanding of both the initial and final states involved in the optical transitions. This is not inconsistent with the billiard-ball picture given above, where we noted that it was necessary to consider Se atoms beyond the nearest-neighbor ligands in order to explain the bifurcation.

In summary, we have shown experimentally that photoemission from  $1T$ -TaSe<sub>2</sub> is quite anisotropic. We have discussed the results from two points of view: (1) a billiard-ball picture which emphasizes the properties of the final states in the optical transitions, and (2) an atomic orbital picture which emphasizes the properties of the initial states. If atomic orbitals are indeed ob-

servable, as suggested above, angular photoemission experiments should be of great value in surface physics. There, one of the outstanding problems is the elucidation of the position and bonding of chemisorbed atoms and molecules. Our experimental results on a layer compound provide strong encouragement for the hope expressed by Gadzuk<sup>9</sup> that surface orbitals should be reflected in the angular distribution of photoelectrons.

We have benefitted from discussions with J. W. Gadzuk, L. F. Mattheiss, E. G. McRae, J. C. Phillips, and J. A. Wilson.

<sup>1</sup>Reviews of ultraviolet photoemission include W. E. Spicer, in *Electronic Density of States*, U. S. National Bureau of Standards Special Publication No. 323, edited by L. H. Bennett (U. S. G. P. O., Washington, D. C., 1971), p. 139; D. E. Eastman, in *Techniques of Metals Research*, edited by E. Passaglia (Interscience, New York, 1972), Vol. 6, Part 1, p. 411.

<sup>2</sup>N. V. Smith and M. M. Traum, *Phys. Rev. Lett.* **31**, 1247 (1973), this paper contains references to previous angular photoemission studies.

<sup>3</sup>J. A. Wilson and A. D. Yoffe, *Advan. Phys.* **18**, 193 (1969); R. A. Bromley and R. B. Murray, *J. Phys. C: Proc. Phys. Soc., London* **5**, 738 (1972); R. B. Murray, R. A. Bromley, and A. D. Yoffe, *ibid.* **5**, 746 (1972); R. A. Bromley, R. B. Murray, and A. D. Yoffe, *ibid.* **5**, 759 (1972); R. B. Murray and A. D. Yoffe, *ibid.* **5**, 3038 (1972); D. R. Edmondson, *Solid State Commun.* **10**, 1085 (1972); J. B. Goodenough, *Mater. Res. Bull.* **3**, 409 (1968); R. Huisman, R. DeJonge, C. Haas, and

F. Jellinek, *J. Solid State Chem.* **3**, 56 (1971).

<sup>4</sup>L. F. Mattheiss, *Phys. Rev. Lett.* **30**, 784 (1973);

R. V. Kasowski, *Phys. Rev. Lett.* **30**, 1175 (1973).

<sup>5</sup>L. F. Mattheiss, *Phys. Rev. B* **8**, 3719 (1973).

<sup>6</sup>J. C. McMenamin and W. E. Spicer, *Phys. Rev. Lett.* **29**, 1501 (1972); R. H. Williams, J. M. Thomas, M. Barber, and N. Alford, *Chem. Phys. Lett.* **17**, 142 (1972); P. M. Williams and F. R. Shepherd, *J. Phys. C: Proc. Phys. Soc., London* **6**, L36 (1973); G. K. Wertheim, F. J. Di Salvo, and D. N. E. Buchanan, *Solid State Commun.* **13**, 1225 (1973).

<sup>7</sup>E. G. McRae, unpublished.

<sup>8</sup>W. L. Schaich and N. W. Ashcroft, *Phys. Rev. B* **3**, 2452 (1971).

<sup>9</sup>J. W. Gadzuk, in *Proceedings of the Thirty-Second Physical Electronics Conference*, Albuquerque, New Mexico, March 1972 (to be published), and unpublished.

<sup>10</sup>We have assumed that the Fermi surface of 1T-TaSe<sub>2</sub> will not differ greatly from that of 1T-TaS<sub>2</sub> as calculated by Mattheiss (Ref. 5).

<sup>11</sup>K. Ganzhorn, *Z. Naturforsch.* **7a**, 291 (1952). The orbitals we have considered are the four equivalent  $sd^3$  hybrids. The  $d$ -like part of one of these orbitals varies as  $xy + yz + zx$ , and (after converting to a coordinate system in which the  $z$  axis is parallel to the  $c$  axis) is identical with the  $d_{x^2}$  orbital of Ref. 3, which has its axis normal to the crystal surface; the axes of the other three orbitals are inclined to the normal and produce broad lobes in the  $\varphi = 0^\circ$ ,  $120^\circ$ , and  $240^\circ$  directions. A ligand-field approximation based on partial but equal occupancy of the  $sd^3$  hybrids represents a rough simulation of the partial occupancy of the  $d_{x^2}$  orbitals indicated by the detailed band calculations in Ref. 5, and also satisfies the threefold rotational symmetry of the crystal.

## Many-Electron Effects for Deep Levels in Solids: The Lattice Vacancy in Diamond

G. D. Watkins and R. P. Messmer

*General Electric Corporate Research and Development, Schenectady, New York 12301*  
(Received 25 March 1974)

The neutral lattice vacancy in diamond is simulated by the clusters C<sub>4</sub>, C<sub>4</sub>H<sub>12</sub>, and C<sub>16</sub>. Many-electron effects within the ground configuration are estimated using the self-consistent-field  $X\alpha$  scattered-wave method. The resulting term splittings are found to decrease precipitously as the size of the cluster increases, in contrast to the conclusions of Coulson and Larkins. It is concluded that in a real crystal these effects should, therefore, be small and that simple one-electron methods represent valid first-order treatments to the problem.

The degree to which simple one-electron methods are valid for treating highly localized defects in solids is a subject of current controversy.<sup>1-4</sup> There is little controversy when one is dealing with a single electron (or hole) trapped in a region otherwise electronically saturated (closed atomic shells, saturated chemical bonds, etc.).

Most color centers in alkali halides, shallow donors or acceptors in semiconductors, etc., fall into this category. However, when more than one electron (or hole) is highly localized, many-electron effects cannot be easily dismissed.

The problem is familiar in atomic structure. The neutral alkali or halogen atoms are relative-